NUMERICAL SIMULATION FOR FLOW SEPARATION AROUND A 2-D AIRFOIL

SHUTIAN DENG, CHAOQUN LIU, HUA SHAN
Department of Mathematics
University of Texas at Arlington, Arlington, TX

Abstract

This paper carries out numerical study of the flow separations around NACA 0012 airfoil at large angles of attack. Flow separation introduces two major effects: sudden loss of lift and generation of aerodynamic noise. These two factors are highly concerned on the aircraft designation. This study gives a detail picture of flow separation.

As the problems caused by flow separation are complicated, the spatial and temporal complexity makes it difficult to access by conventional experiment methods. In the presented work, the numerical investigation results from solving the time-dependent Navier-Stockes equations in the generalized curvilinear coordinates. Using a fourth order centered compact scheme for spatial discretization facilitates high resolution of the flow field, which will be neglected if using low-order numerical schemes. To avoid possible non-physical wave reflection, the non-reflecting boundary conditions are used at far-field and outlet boundary.

Complex flow separation, vortex shedding, vortex merging, and vortex paring are observed in the computational results. The main purpose of this paper is to provide more detailed information of the flow separation.

1. Introduction

Flow separation around airfoil receives highly concerned from the researchers. Shih et al.(1992) had pointed out that the understanding of this problem needs to make a step forward from qualitative conjecture to quantitative measurement of the instantaneous flow field. Shih et al (1995) investigated the unsteady flow past a NACA 0012 airfoil in pitching-up motion experimentally. They carried out the experiment at a Reynolds number of 5000 using PIDV method. Instantaneous velocity field data at different times have been obtained over the whole flow field. They drew the conclusion that boundary-layer separation near the airfoil leading edge leads to the formation of a vortical structure. The evolution of the vortex along the upper surface dominates the aerodynamic performance of the airfoil. Complete stall emerges when the boundary layer near the leading edge detaches

from the airfoil, under the influence of the vortex. Furthermore in 1995 they studied the stall process using a water towing tank facility, and found that near the leading edge large vortical structures emerge as a consequence of Van Dommelen and Shen type separation and a local vorticity accumulation. They pointed out that the trailing edge only play a secondary role on the dynamic stall process.

Tenaud & Phuoc (1997) used large eddy simulation (LES) to study this problem. They described that three flow fields can be distinguished according to different flow structures. Near the leading edge, vortex shedding due to separation of the boundary layer is dominant. In the second area, which is the middle part of the upper surface of the airfoil, the eddy structures grow and move downstream. The last field is close to the trailing edge, where the alternate vortices are created.

This work focuses on numerical simulation of flow separation around a NACA 0012 airfoil at a 16 angle of attack. From the previous understanding of experimental and numerical investigation of this problem, it is known that large vortices are generated and shed from the leading edge, thus leads to fluctuation of pressure and the lift lost. But the detail of this process is still unclear, the main purpose of this work is to give detailed picture of flow separation structures using a high-order and high-resolution approach.

2. Basic Equation And Numerical Methods

The governing equations are the two-dimensional compressible Navier-Stocks equations in the generalized curvilinear ξ-η coordinates, and in a conservative form:

$$\frac{1}{J}\frac{\partial Q}{\partial t}+\frac{\partial (E-E_v)}{\partial \xi}+\frac{\partial (F-F_v)}{\partial \eta}=0 \tag{1}$$

where flux vectors F, E, E_v, F_v are:

$$Q=\begin{bmatrix}\rho\\ \rho u\\ \rho v\\ e\end{bmatrix} \quad E=\frac{1}{J}\begin{bmatrix}\rho U\\ \rho uU+p\xi_x\\ \rho vU+p\xi_y\\ U(e+p)\end{bmatrix} \quad F=\frac{1}{J}\begin{bmatrix}\rho V\\ \rho uV+p\eta_x\\ \rho vV+p\eta_y\\ V(e+p)\end{bmatrix}$$

$$E_v=\frac{1}{J}\begin{bmatrix}0\\ \tau_{xx}\xi_x+\tau_{yx}\xi_y\\ \tau_{xy}\xi_x+\tau_{yy}\xi_y\\ q_x\xi_x+q_y\xi_y\end{bmatrix} \quad F_v=\frac{1}{J}\begin{bmatrix}0\\ \tau_{xx}\eta_x+\tau_{yx}\eta_y\\ \tau_{xy}\eta_x+\tau_{yy}\eta_y\\ q_x\eta_x+q_y\eta_y\end{bmatrix}$$

Where J is the Jacobian of the coordinate transformation, and $\xi_x, \xi_y, \eta_x, \eta_y$ are coordinate transformation metrics. ρ is density, p is pressure, u and v are components of velocity. $U = u\xi_x + v\xi_y$, $V = u\eta_x + v\eta_y$. e is the total energy. The components of viscous stress and heat flux are denoted by $\tau_{xx}, \tau_{yy}, \tau_{xy}$ and q_x, q_y, respectively.

The second order Euler Backward scheme is applied to solve Eq. (1), that is,

$$\frac{3Q^{n+1} - 4Q^n + Q^{n-1}}{2J\Delta t} + \frac{\partial(E^{n+1} - E_v^{n+1})}{\partial\xi} + \frac{\partial(F^{n+1} - F_v^{n+1})}{\partial\eta} = 0 \tag{2}$$

Q^{n+1} is estimated iteratively as: $Q^{n+1} = Q^p + \delta Q^p$, $\delta Q^p = Q^{p+1} - Q^p$
Flux vectors are linearized by the local Taylor expansion about Q as following:

$$E^{n+1} \approx E^p + A^p \delta Q^p, \quad F^{n+1} \approx F^p + B^p \delta Q^p$$

Now equation (2) turns into:

$$[\frac{3}{2} I + \Delta t J (D_\xi A + D_\eta B)]\delta Q^p = R \tag{3}$$

Where $R = -(\frac{3}{2}Q^p - 2Q^n + \frac{1}{2}Q^{n-1}) - \Delta t J [D_\xi (E - E_v) + D_\eta (F - F_v)]^p$

The superscript p stands for iteration step. D_ξ and D_η are partial differential operators in the ξ and η directions, respectively. The right hand side of Eq. (3) is discretized using the fourth-order compact scheme. A sixth-order compact filter is used to depress the numerical oscillation. The left hand side of Eq. (3) is discretized following the LU-SGS method (Yoon & Kwak, 1992). Then the finite difference expression of Eq. (3) can be written as:

$$\left[\frac{2}{3} I + \Delta t J (r_A + r_B) I\right] \delta Q_{i,j}^p = R_{i,j}^p -$$

$$\Delta t J \left[A^- \delta Q_{i+1,j}^p - A^+ \delta Q_{i-1,j}^p + B^- \delta Q_{i,j+1}^p - B^- \delta Q_{i,j-1}^p\right]$$

Where $A^\pm = \frac{1}{2}[A \pm r_A I]$, $B^\pm = \frac{1}{2}[B \pm r_B I]$, and $A = A^+ + A^-$,

$$B = B^+ + B^-, \quad A = \frac{\partial E}{\partial Q}, \quad B = \frac{\partial F}{\partial Q},$$

$$r_{A,B} = k \max[|\lambda(A,B)|] + \nu,$$

$$\nu = \max[\frac{\mu}{(\gamma - 1) M_r^2 R_e P_r}, \frac{4}{3}\frac{\mu}{R_e}].$$

For subsonic flow, u, v, T are prescribed at the upstream boundary, p is obtained by solving the modified N-S equation based on characteristic analysis. On the far-field and out-flow boundary, the non-reflecting boundary conditions are

applied. Adiabatic, non-slipping condition is used for the wall boundary. All equations of boundary conditions are solved implicitly with internal points. Specific details of boundary treatment can be found in Jiang et al. (1999)

3. Grid Generation

A grid generation method first proposed by Spekreijse (1995) is used to generate the C-type grids. The grid generation method is a composite method, which consist of an algebraic transformation and an elliptic transformation. The algebraic transformation maps the computational space onto a parameter space, and the elliptic transformation maps the parameter space onto the physical domain by solving a set of Poisson equations. The orthogonality of grids on the surface and near the boundary is achieved by re-configuration of the algebraic transformation. The grid numbers are 841 in the ξ direction, and 141 in the η direction. The overview of the C-grid and grid near the airfoil surface are displayed in Figure 1(a) and (b).

4. Computational Result

The flow field around an NACA-0012 airfoil is analyzed by solving the Navier-Stocks equations using the finite difference scheme. Flow separation at a large angle of attack ($\alpha = 16^\circ$) has been studied using a high-resolution numerical simulation. In this case, the fluid flow around the airfoil becomes very unstable and different eddy structures are formed in the vicinity of the airfoil. The Reynolds number based on the chord length and the free-stream velocity is 5×10^5, the free stream Mach number is 0.4. The angle of attack is 16 °. During the computation, the flow field is recorded every 1000 time steps, and the time step is approximately $1.768\times10^{-4} L/U_\infty$. Figure 2 shows the contours of the instantaneous spanwise voriticity. The time interval between each of those 15 pictures is about $0.7072L/U_\infty$. From those figures we can see that flow separation process start at the leading edge and the leading edge vortices continue to shed and convect downstream. In Figure 2(c), a separation bubble can be observed on the upper surface of the airfoil near the leading edge. A chain of vortical structures appear on the upper surface of the airfoil, which is more clear in Figure 2(h). The vortices shedding from the leading-edge rotate in the clockwise direction. Near the surface of the airfoil, a layer of reversed vorticity is induced by the vortices shedding from the leading-edge. The interactions between the positive and negative vorticity leads to the vortex pairing. The merging of vortices rotating in the same direction is also observed, e.g. in Figure 2(j). A vortex, which first appears at the trailing edge of airfoil in Figure 2(a), grows as it is carried downstream by the mean flow, as shown in Figure 2(b), (c), and (d). In Figure 2(d), along the shear layer starting from the trailing edge, a series of small vortical structures are generated as a result of the Kelvin-Helmholtz instability. These small structures are also visible in Figure 2(e), (f), (g), and (h).

5. Conclusions

Detailed numerical simulation has been carried out by solving Navier-Stocks equations in the generalized curvilinear coordinates to study the separated flow around an NACA 0012 airfoil at large angle of attack. By using a fourth–order centered compact scheme for spatial discretization, the small–scale vortical structures are resolved, which will dissipate if low-order numerical schemes are used. Non-reflecting boundary conditions are imposed at the far field and outlet boundaries to avoid possible non-physical wave reflection.

The numerical simulation results clearly describe the flow separation process at the upper surface of the airfoil. The phenomena of the leading-edge separation, vortex shedding, vortex merging, vortex pairing, and formation and shedding of large-scale trailing edge vortex are displayed and discussed in detail. The small-scale vortices associated with the Kelvin-Helmholtz instability are also observed along the shear layer near the trailing-edge. These phenomena are in food agreement with the experimental results obtained by Shih, et al (1992,1995) and Yoshifumi et al (1986).

Reference:

[1] L. Jiang, H. Shan, C. Liu and M. R. Visbal 1999. Non-reflecting boundary condition in curvilinear coordinates, Second AFOSR International Conference on DNS/LES, Rutgers, New Jersey, June 7-9

[2] S. K. LeLe 1992. Compact finite difference schemes with spetral-like resolution. Journal of Computational Physics. 103 ,P 16-42

[3] C. Shih, L. Lourenco, L. Van Dommelen and A. Krothapalli 1992. Unsteady flow past an airfoil pitching at a constant rate. AIAA Journal, 30(5), P 1153-1161

[4] C. Shih, L. Lourenco, and A. Krothapalli 1995. Investigation of flow ar leading and trailing edge of pitching-up airfoil. AIAA Journal, 30(5), P 1369-1376

[5] S. P. Spekreijse 1995. Elliptic grid generation based on Laplace equations and algebraic transformation. Journal of Computational Physics. 118 ,P 38-61

[6] C. Tenaud and L. T. Phuoc 1997. Large eddy simulation of unsteady, compressible, separated flow around NACA 0012 airfoil. Lecture Notes in Physics 490, P424-429

[7] J. F. Thompson, Z. U. A. Warsi and C. W. Mastin 1985. Numerical Grid Generation: Foundations and Applications. Elsevier, New York

[8] L. Van Dommelen and Shen 1980. The Spontaneous generation of singularity in a separating laminar boundary layer. Journal of Computational Physics.38,P 125-140

[9] L. Van Dommelen and S. J. Cowsley 1990. On the Lagrangian description of unsteady boundary later, Part 1: General theory. J. Fluid Mech., 210 P593-626

[10] J-Z. Wu, X. Lu, A. G. Denny, M. Fan and J-M Wu 1999. Post-stall lfow control on an airfoil by local unsteady forcing. J. Fluid Mech., 371 P 21-58

[11] S. Yoon and D. Kwak 1992. Implicit Navier-Stocks solver for three-dimensional compressible flows. AIAA Journal, 30(5), P 2653-2659

[13] S. P. Spekreijse 1995. Elliptic grid generation based on Laplace equations and algebraic transformation. J. Comp. Phys., 118, P 38-61

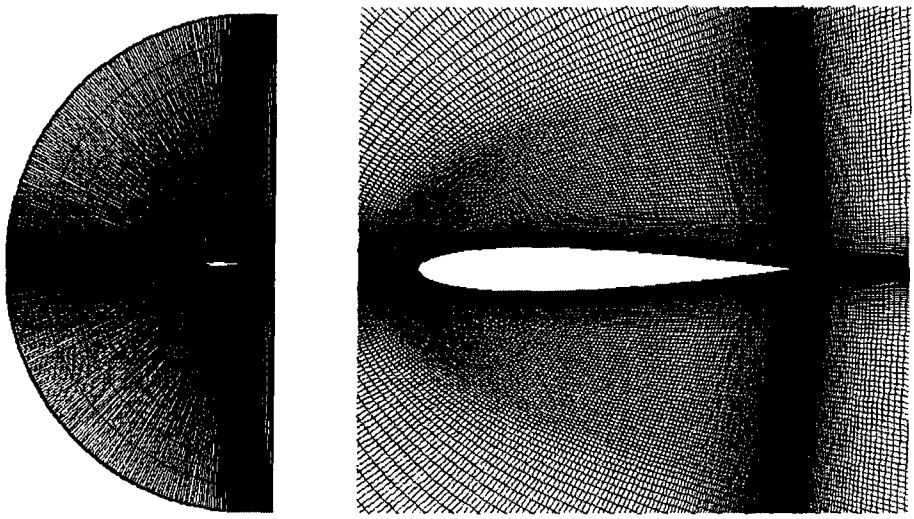

(a) overview of the grids (b) grids near airfoil surface

Figure 1. C-grid around an NACA 0012 airfoil

(a)

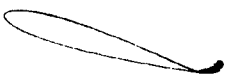

(b)

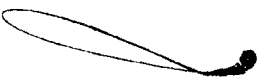

(c)

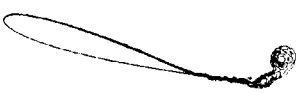

(d)

(e)

(f)

(g)

(h)

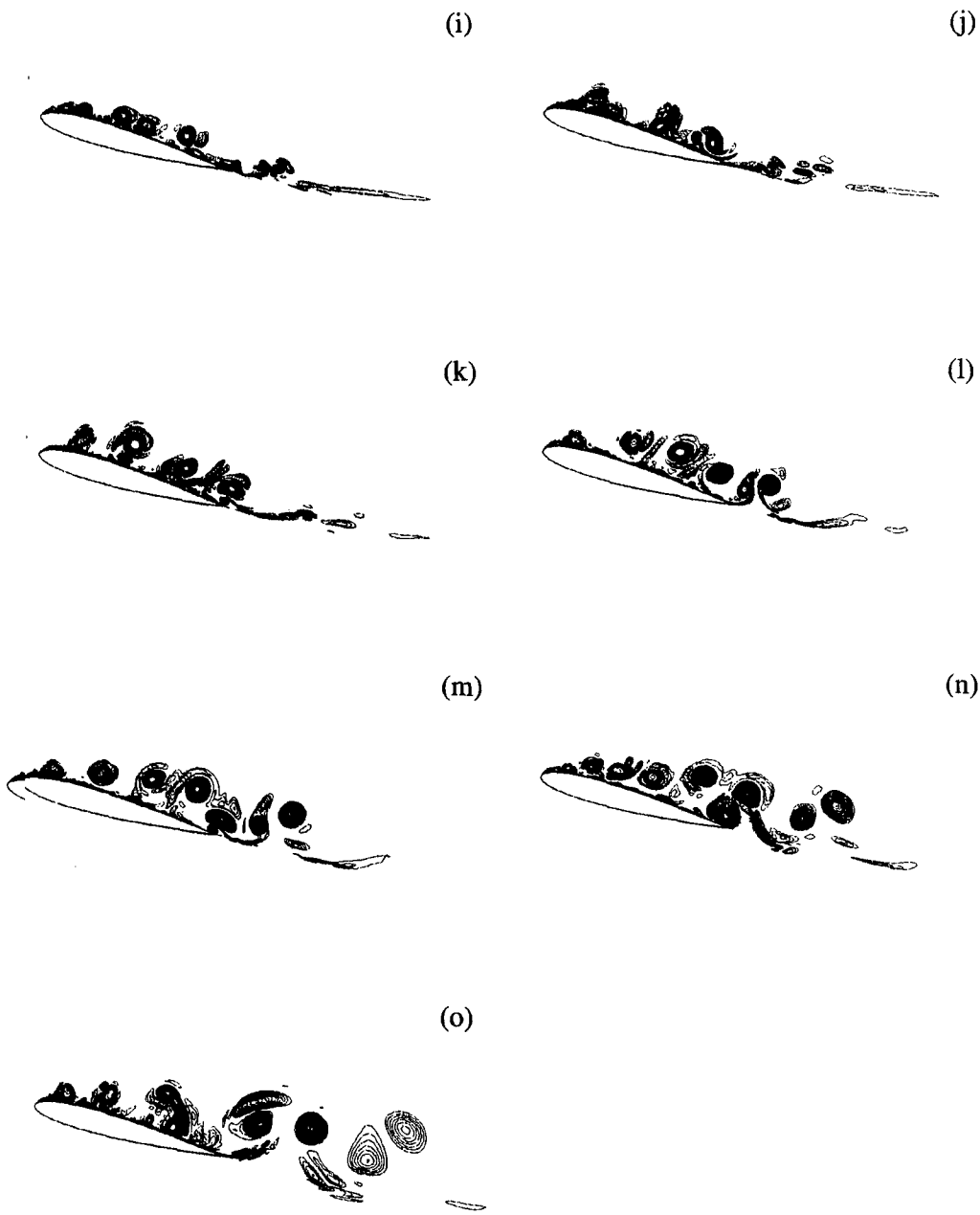

Figure 2. Contours of instantaneous spanwise vorticity at different time